TOPICAL REVIEW • OPEN ACCESS

Overlooked cooling effects of albedo in terrestrial ecosystems

To cite this article: Jiquan Chen *et al* 2024 *Environ. Res. Lett.* 19 093001

View the article online for updates and enhancements.

ENVIRONMENTAL RESEARCH
LETTERS

TOPICAL REVIEW

Overlooked cooling effects of albedo in terrestrial ecosystems

Jiquan Chen[1,2,3,*] , Cheyenne Lei[2,4] , Housen Chu[5], Xianglan Li[2,6], Margaret Torn[5], Ying-Ping Wang[7], Pietro Sciusco[2,8] and G Philip Robertson[3,9,10]

1   Center for Global Change and Earth Observations, Michigan State University, East Lansing, MI, United States of America
2   Department of Geography, Environment & Spatial Sciences, Michigan State University, East Lansing, MI, United States of America
3   DOE Great Lakes Bioenergy Research Center, Michigan State University, East Lansing, MI, United States of America
4   Institute for Global Change Biology, School for Environment and Sustainability, University of Michigan, Ann Arbor, MI, United States of America
5   Lawrence Berkeley National Laboratory, Berkeley, CA, United States of America
6   College of Global Change and Earth System Sciences, Faculty of Geographical Science, Beijing Normal University, Beijing, People's Republic of China
7   CSIRO Environment, Private Bag 10, Clayton South, VIC 3169, Australia
8   Planetek Italia S.r.l., Bari 70132, Italy
9   Department of Plant, Soil and Microbial Sciences, Michigan State University, East Lansing, MI, United States of America
10   W. K. Kellogg Biological Station, Michigan State University, Hickory Corners, MI, United States of America
*   Author to whom any correspondence should be addressed.

E-mail: jqchen@msu.edu

Abstract

Radiative forcing (RF) resulting from changes in surface albedo is increasingly recognized as a significant driver of global climate change but has not been adequately estimated, including by Intergovernmental Panel on Climate Change (IPCC) assessment reports, compared with other warming agents. Here, we first present the physical foundation for modeling albedo-induced RF and the consequent global warming impact ($GWI_{\Delta\alpha}$). We then highlight the shortcomings of available current databases and methodologies for calculating $GWI_{\Delta\alpha}$ at multiple temporal scales. There is a clear lack of comprehensive *in situ* measurements of albedo due to sparse geographic coverage of ground-based stations, whereas estimates from satellites suffer from biases due to the limited frequency of image collection, and estimates from earth system models (ESMs) suffer from very coarse spatial resolution land cover maps and associated albedo values in pre-determined lookup tables. Field measurements of albedo show large differences by ecosystem type and large diurnal and seasonal changes. As indicated from our findings in southwest Michigan, $GWI_{\Delta\alpha}$ is substantial, exceeding the $RF_{\Delta\alpha}$ values of IPCC reports. Inclusion of $GWI_{\Delta\alpha}$ to landowners and carbon credit markets for specific management practices are needed in future policies. We further identify four pressing research priorities: developing a comprehensive albedo database, pinpointing accurate reference sites within managed landscapes, refining algorithms for remote sensing of albedo by integrating geostationary and other orbital satellites, and integrating the $GWI_{\Delta\alpha}$ component into future ESMs.

1. Introduction

Since its inclusion in the 3rd Assessment Report (AR3) of the Intergovernmental Panel on Climate Change (IPCC) in 2001 (IPCC (Intergovernmental Panel on Climate Change) 2001), the radiative forcing (RF) resulting from changes in surface albedo (RF_α) due to land use and land cover changes (LULCC) has been recognized as a significant driver of global climate warming/cooling (Davin *et al* 2007, Ghimire *et al* 2014, Sieber *et al* 2019, Smith *et al* 2020). The IPCC 6th Assessment Report (AR6) estimates a global average RF_α of 0.20 ± 0.10 W m^{-2} (Masson-Delmotte *et al* 2021, IPCC (Intergovernmental Panel on Climate Change) 2022), or 9.3% of the RF attributed to increasing

CO_2 concentrations (2.16 ± 0.25 W m^{-2}), which is similar to the RF of historical N_2O and CH_4 emissions (0.21 ± 0.30 W m^{-2}). However, a growing body of research on RF_α in terrestrial ecosystems suggests that the global RF_α value is significantly higher than those in IPCC's assessment reports (Burakowski *et al* 2018, Carrer *et al* 2018, Sciusco *et al* 2020, Ouyang *et al* 2022, Graf *et al* 2023, Lei *et al* 2023, Salisbury *et al* 2023, Zhu *et al* 2024a, 2024b). For instance, Sciusco *et al* (2020) reported a CO_2-equivalent mitigation value ranging from 23% to 52% of carbon sequestration from agriculture-dominated watershed compared to the original forest-dominated landscapes in southwest Michigan, USA. Carrer *et al* (2018) quantified RF_a from cropland conversion in Europe and found that the albedo change contributed 10%–13% to the total RF. Other recent studies also concluded that previous reports significantly underestimated the contribution of RF_α to total RF (Lee *et al* 2011, Sieber *et al* 2019, Abraha *et al* 2021, Chen *et al* 2021, Ouyang *et al* 2022, Sciusco *et al* 2022, Lei *et al* 2024), despite substantial regional variations in albedo and RF due to disparities in LULCC patterns among regions, climate variability, and external forcing factors, as well as intra- and inter-annual fluctuations.

Regrettably and surprisingly, there has been limited research on albedo changes with LULCC, as well as the corresponding modeling of the RF due to changed albedo ($RF_{\Delta\alpha}$). This limitation hinders our understanding of whether $RF_{\Delta\alpha}$ contributes a significantly larger proportion to the overall RF across terrestrial ecosystems than previously believed. From a policy perspective, there has been a failure to recognize and provide credits to land owners, including farmers, who actively contribute to climate regulation through sustainable management practices. These practices include cover cropping, timely tillage, residue management, and crop selection. While these actions contribute to soil protection and restoration by enhancing soil organic carbon, they can also affect albedo, potentially leading to cooling or warming effects. These practices involve increasing the reflectivity of cultivated lands compared to their original land cover or more typical management and can have a cooling effect on climate due to elevated albedo. Here we (1) present the challenges associated with accurately estimating $RF_{\Delta\alpha}$; (2) examine the potential pitfalls and opportunities in modeling $RF_{\Delta\alpha}$; and (3) emphasize the urgent need for integrating $RF_{\Delta\alpha}$ into the overall assessment of global warming impact (GWI) for local ecosystems, thus necessitating revisions to existing policies. By addressing these objectives, we aim to advocate for its inclusion in comprehensive assessments of ecosystem-level impacts, as well as the formulation of appropriate policy measures.

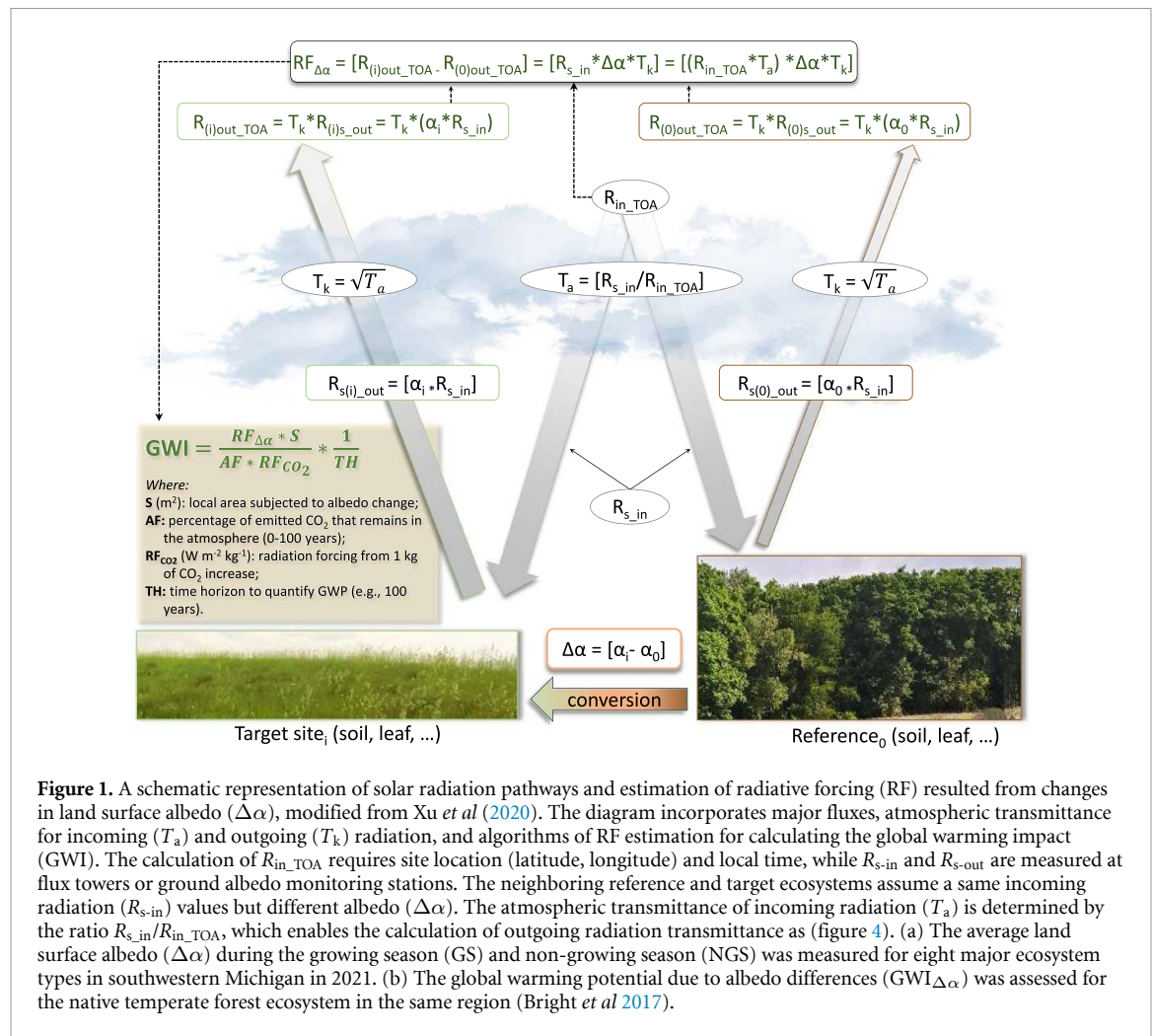## 2. Challenges in estimating $RF_{\Delta\alpha}$ and $GWI_{\Delta\alpha}$

Solar radiation, predominantly consisting of short-wave radiation, passes through an atmosphere that varies in depth and composition due to factors such as cloud cover, water vapor, and aerosol concentration. The land surface albedo (α) refers to the fraction of incoming solar radiation that is not absorbed by the surface but rather is reflected by the surface back to space (figure 1). The amount of outgoing shortwave radiation is influenced primarily by land surface properties, such as vegetation type, leaf area, and soil moisture. Canopy structure plays a crucial role, where deeper and more intricate canopies (e.g. forests) tend to absorb more shortwave radiation (low albedo) compared to simpler, shallower canopies like crops and grasslands (high albedo). While the atmospheric conditions remain generally the same for incoming and outgoing radiation, there are differences in the layering features. Incoming radiation passes through a thin-to-thick atmosphere, whereas outgoing radiation traverses a reversed layering pattern. As a result, the atmospheric transmittance (T_k) for outgoing radiation reflected by the Earth's surface is higher than that for incoming radiation (T_a) (Bright and Lund 2021). While T_a can be reliably quantified based on measurements of radiation at the top of the atmosphere (R_{in_toa}) and at the ground level (R_{s_in}), estimating T_k values is challenging due to atmospheric composition and layering complexities.

Several methods have been proposed for calculating $RF_{\Delta\alpha}$ of an ecosystem (e.g. Bright and Lund 2021, Lei *et al* 2023), with a more widely used foundation of:

$$RF_{\Delta\alpha} = -\frac{1}{N}\sum_{N=1}^{N}[R_{s\_in} \cdot \Delta\alpha \cdot T_k] \qquad (1)$$

where $\Delta\alpha$ is the mean albedo difference between the target ecosystem and a reference land cover over a specific time period, $R_{s\text{-}in}$ is the incoming solar radiation at the land surface (top of canopy) that can be measured with pyranometers, N is the number of samplings of the integration period (e.g. hours of a day, or days of a month), and T_k is the upward atmospheric transmittance.

Processes influencing $RF_{\Delta\alpha}$ and its calculation are illustrated in figure 1. For the calculations, R_{s_out} is a measured quantity and R_{in_TOA} is a theoretical number calculated based on the solar constant (1.37 kW m^{-2}), latitude, longitude, and local time (Chen 2021). For a study ecosystem, $\Delta\alpha$ and T_a can

Figure 1. A schematic representation of solar radiation pathways and estimation of radiative forcing (RF) resulted from changes in land surface albedo ($\Delta\alpha$), modified from Xu *et al* (2020). The diagram incorporates major fluxes, atmospheric transmittance for incoming (T_a) and outgoing (T_k) radiation, and algorithms of RF estimation for calculating the global warming impact (GWI). The calculation of R_{in_TOA} requires site location (latitude, longitude) and local time, while $R_{s\text{-}in}$ and $R_{s\text{-}out}$ are measured at flux towers or ground albedo monitoring stations. The neighboring reference and target ecosystems assume a same incoming radiation ($R_{s\text{-}in}$) values but different albedo ($\Delta\alpha$). The atmospheric transmittance of incoming radiation (T_a) is determined by the ratio R_{s_in}/R_{in_TOA}, which enables the calculation of outgoing radiation transmittance as (figure 4). (a) The average land surface albedo ($\Delta\alpha$) during the growing season (GS) and non-growing season (NGS) was measured for eight major ecosystem types in southwestern Michigan in 2021. (b) The global warming potential due to albedo differences ($\text{GWI}_{\Delta\alpha}$) was assessed for the native temperate forest ecosystem in the same region (Bright *et al* 2017).

be directly measured (**S-1**). GWI of CO_2 equivalent, for example, is calculated as:

$$\text{GWI} = \frac{\text{RF}_{\Delta\alpha} * S}{\text{AF} * \text{RF}_{CO_2}} * \frac{1}{\text{TH}} \qquad (2)$$

where S (m²) is the local area subjected to albedo change, AF is the percentage of emitted CO_2 that remains in the atmosphere (e.g. 0–100 years); RF_{CO2} (W m⁻² kg⁻¹) is the radiation forcing from 1 kg of CO_2 increase, and TH is time horizon to quantify GWI (e.g. 100 years). Algorithms for converting $\text{RF}_{\Delta\alpha}$ to GWI in CO_2-equivalent, biomass, carbon, and CO_2-forcing-equivalent emission (CO_2-fe) have been proposed and successfully applied for various purposes (Bright *et al* 2017, Jenkins *et al* 2018, Sieber *et al* 2019, IPCC (Intergovernmental Panel on Climate Change) 2022, Zhu *et al* 2024a, 2024b, including a spreadsheet model in Chen (2021). Negative values of both $\text{RF}_{\Delta\alpha}$ and $\text{GWI}_{\Delta\alpha}$ indicate cooling effects due to elevated surface albedo.

It is important to highlight that even minor changes in albedo ($\Delta\alpha$) can lead to significant change in radiative forcing ($\text{RF}_{\Delta\alpha}$). For instance,

Chen (2021) demonstrated that a mere 1% increase in the albedo of crops such as corn, sorghum, and switchgrass, resulting from their conversion from native forests in southwest Michigan, USA, can generate a cooling effect equivalent to $\text{GWI}_{\Delta\alpha}$ of approximately 0.5 Mg C ha⁻¹ yr⁻¹ over a 100 year time horizon, following the Kyoto protocol. This cooling effect is substantial when considering the carbon sequestration potential of forests, which ranges from approximately 2.5–3.0 Mg C ha⁻¹ yr⁻¹ (Xiao *et al* 2008).

The calculation of $\text{RF}_{\Delta\alpha}$ (equation (1)) requires three essential parameters ($R_{s\text{-}in}$, $\Delta\alpha$, and T_k), each presenting unique challenges arising from distinct physical and ecological processes. $R_{s\text{-}in}$ and $R_{s\text{-}out}$ can be directly measured and recorded using modern radiometers and dataloggers. Extrapolation, however, is more challenging. $R_{s\text{-}in}$ can reasonably be extrapolated to larger spatial scales (e.g. several kilometers) as the atmospheric conditions at this scale are relatively homogeneous. However, extrapolating R_{s_in} across temporal scales poses significant challenges due to the sensitivity of incoming radiation to atmospheric depth, composition, and layering. By measuring R_{s_in}, the *in situ* value of T_a at a specific time can be reliably calculated. Likewise, extrapolating
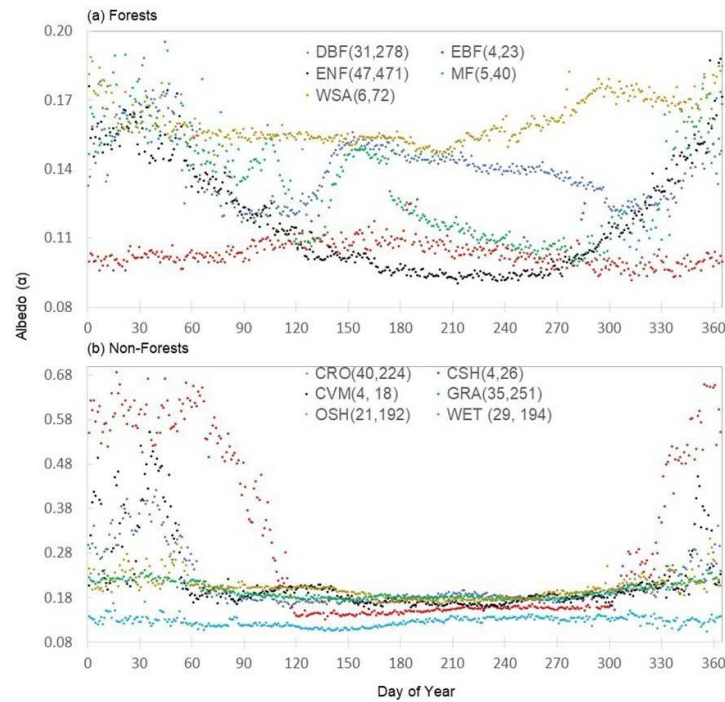
Figure 2. (a) Daily time series of midday albedo (11:00–13:00 h local time) were analyzed from selected AmeriFlux sites (**SI-2**), grouped as forest clusters based on IGBP land cover classifications. Each time series represents a composite of data from all available years and sites. (b) Daily time series of midday albedo (11:00–13:00 h local time) for non-forests. Each time series represents a composite of data from all available site and site-year. The first numbers in parentheses indicates the total number of sites used for calculating the average albedo values, and the second number indicates the total site-year used for each type. Cover types with less than 4 tower sites are excluded.

R_{s_out} across temporal and spatial scales encounters many challenges, along with additional complexities related to vegetation characteristics, geographic location, time, and other factors (Shao *et al* 2014, Sieber *et al* 2019).

Estimating T_k also poses considerable difficulties. Firstly, there is a lack of outgoing radiation measurements at the top of the atmosphere. Secondly, despite other studies that assume the upward and downward atmospheric transmittances to be equal (e.g. Carrer *et al* 2018, Sciusco *et al* 2020, 2022), T_k cannot be assumed to be the same as T_a due to alterations in spectral composition. Finally, the reversed layering of the atmosphere further complicates T_k estimation (S-1). While an ideal solution would involve a well-parameterized radiation transport model that considers detailed atmospheric layering and composition, constructing such a model for all land areas is not feasible. Fortunately, there are observed high correlations between T_a and T_k. Bright and Lund (2021) concluded that the best estimate of T_k is. It is important to note that T_a exhibits significant variations with solar zenith angle (SZA) and decreases with increasing atmospheric depth according to Beer's law and is also influenced by factors such as clouds, aerosols, and other atmospheric gases. Global Daily R_{s_in} is available at the Downward Surface Shortwave Flux (DIDSSF-R, https://landsaf.ipma.pt/en/products/longwave-shortwave-radiation/didssf-cdr/).

Likewise, estimating $\Delta\alpha$ and its spatiotemporal changes presents significant challenges, particularly when modeling the GWI caused by LULCC. This difficulty arises primarily from the complex and multifactorial influences on reflectance (R_{s_out}). Extensive literature has documented the various factors influencing albedo, including geographic position (e.g. latitude, topography), time (e.g. hour of the day, day of the year), vegetation type, canopy composition and structure (e.g. canopy height, leaf amount, horizontal and vertical distribution, coverage), soil moisture, and snow cover (Jarvis 1976).

During periods of low SZA, such as morning and late afternoon, deeper canopies tend to reflect more visible light while absorbing more infrared/near-infrared radiation, although the visible spectrum dominates the total energy amount (Chen 2021). In general, denser canopies with high leaf area index (LAI) and taller structures absorb more incoming radiation, leading to lower albedo values. Based on direct measurements of albedo from 906 site-year data at 286 eddy covariance flux towers within the terrestrial areas of AmeriFlux (figure 2), forests generally exhibit lower albedo values (0.104–0.160) as compared to non-forested areas (0.126–0.314). Among forested ecosystems, Evergreen Broadleaf Forests have the highest albedo values, while Deciduous Broadleaf Forests (DBFs) have the lowest (figure 2(a)). For non-forest ecosystems, Wetlands and Closed Shrublands
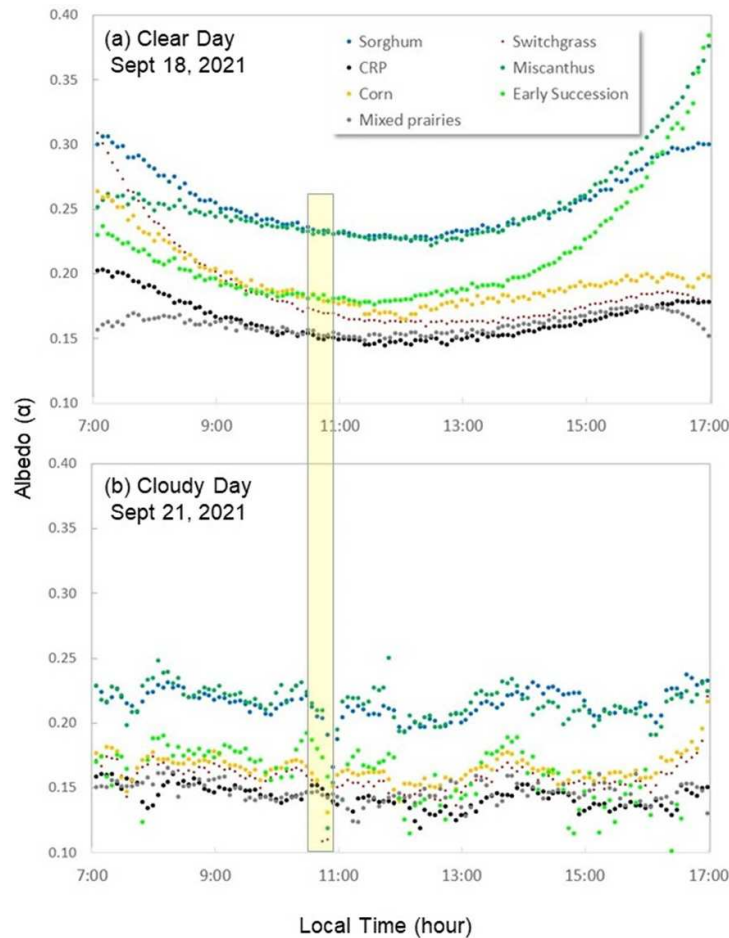
Figure 3. Diurnal changes and variations in land surface albedo under clear (a) and cloudy (b) sky conditions for seven bioenergy crops at the Kellogg Biological Station (KBS) in Southwest Michigan, USA. The yellow shaded area on the bar graph represents the local time (∼10:30 h) when the Landsat/Terra satellites pass over the study sites.

show the lowest and highest albedo values, respectively (figure 2(b)). The differences in albedo values among different land cover types are typically more pronounced during the winter months compared to the summer months, except for DBF. Understanding the differences among land cover types and their associated seasonal changes is crucial when considering management alternatives and policy revisions to include $GWI_{\Delta\alpha}$ in quantifying the comprehensive impact of ecosystem attributes on climate.

There are also distinct diurnal changes in albedo, although their appearance depends on atmospheric conditions such as cloud cover and varies among different land cover types that have distinct surface properties. By utilizing ground-based albedo measurements from seven experimental crops at the Kellogg Biological Station Long-term Ecological Research site (KBS LTER) in southwest Michigan (figure 3), we confirm that albedo reaches its lowest point around midday, exhibiting an imperfect symmetric diurnal pattern. More radiation reaches the ground due to the shorter atmospheric path around mid-day than other times. The incoming solar radiation consists of a substantial amount of IR/NIR radiation, which

is absorbed relatively less by plants, resulting in a higher reflection portion. In the early morning or late afternoon, when SZA is low, a higher amount of radiation is reflected based on the cosine law (Chen 2021). Notably, despite the experimental plots being located within a 500-meter radius, there are significant differences in albedo among the different land cover types and their diurnal changes, indicating variations due to specific cover types. On a clear day, such as 18 September 2021, a restored prairie system exhibited the lowest albedo value (0.150) and the smallest diurnal fluctuations, while energy sorghum (*Sorghum bicolor*) and miscanthus (*Miscanthus × gigantea*) stands showed much higher albedo (0.260 and 0.257, respectively) throughout the day, resulting in an average albedo difference of approximately 0.11 compared to restored prairies. This magnitude of difference can lead to substantial $RF_{\Delta\alpha}$ for these crops (Chen 2021). However, on a cloudy day (three days later on 21 September 2023), the diurnal changes in albedo were not apparent, with albedo levels similar to noon values on a clear day (figure 3(b)) for these cover types, and sorghum and miscanthus still maintaining higher

albedo values. Under cloudy conditions, radiation mostly consists of scattered irradiation by the clouds, resulting in minimal diurnal variations and a near constant albedo throughout the day. On cloudy days the portion of IR/NIR radiation passing through the atmosphere and canopies is also similar throughout the day, suggesting that albedo during early and late hours will be reduced to the same level as at noon. Regarding the $RF_{\Delta\alpha}$ of these crops, their daily sum will subsequently be reduced because albedo differences at noon appear the smallest throughout the daytime hours (figure 3(a)). A plausible observation is that albedo values between ground measurements and satellite records around noon seem similar. Nonetheless, modeling these reductions in $RF_{\Delta\alpha}$ (and $GWI_{\Delta\alpha}$) with variable cloud cover remains a necessary future endeavor.

3. Limitations in current estimates of albedo

Our ability to assess spatial and temporal changes in albedo relies on direct measurements using two-way radiometers, remote sensing of land surface reflectance, and earth system modeling. However, there is currently a lack of comprehensive and representative *in situ* measurements of land surface albedo due to the limited field of view and sparse geographic coverage of ground-based instruments. While tower-based measurements are available in several networks (i.e. SUFRAD, BSRN, FLUXNET), many surface types are underrepresented (Chu *et al* 2017). Despite the higher albedo and significant changes observed in high latitude regions, there is a limited number of towers in these regions within the FLUXNET network (figure 2). A more challenging aspect in calculating $\Delta\alpha$ arises from the need to determine the reference albedo, i.e. the land cover type prior to land conversion (Zhu *et al* 2024a). Our analysis of all AmeriFlux stations, for example, revealed only a limited number of sites with nearby reference areas for which surface albedo are measured. Historical reference sites are important for documenting long-term climate change impacts of $\Delta\alpha$ and contemporary reference sites that represent alternative land use practices are valuable for documenting the impact of current land use choices and potential influences on future policies.

Albedo estimates from orbiting satellites suffer from biases due to the limited frequency of image collection, typically once a day under clear sky conditions (Schaaf *et al* 2002, Wang *et al* 2017), albeit geostationary satellites have the potential to evaluate continuous changes in albedo (Ceamanos *et al* 2019). This trade-off between temporal and spatial resolutions poses a significant challenge. Moreover, a critical issue arises from the fact that estimating albedo from satellites, such as MODIS and Landsat, represents a snapshot equivalent to their overpass local time

(i.e. around noon for the southwest Michigan site in figure 3). For instance, the Landsat and Sentinel satellites, widely used in land cover studies, pass local time at KBS LTER at approximately 10:00–10:30 h, corresponding to a solar altitude of around 60°. However, during this time period, the albedo is lower compared to the period before 10:00 h and after 14:00 h. Therefore, on 18 September 2021 (figure 3(a)), albedo estimates from these satellites would be 24% lower than the daily averages for the seven cover types examined. Consequently, $GWI_{\Delta\alpha}$ calculations based on these satellite measurements would overlook the albedo values in the early morning and late afternoon, introducing similar biases (Cai *et al* 2016, He *et al* 2018, Sieber *et al* 2019, Sciusco *et al* 2022).

Finally, earth system models (ESMs) offer rough estimates of albedo at very coarse spatial resolutions by empirically defining optical properties using lookup tables, such as 'soil colors,' 'plant functional type (PFT),' and 'coverage of bare soils and snow' (Lawrence *et al* 2019). These tables are based on previous works of Sellers (1985) and Bonan (1996), where dynamic independent variables like canopy properties (e.g. species, height, LAI, phenology) are incorporated (Bright *et al* 2015, Tian *et al* 2017, Tian *et al* 2018). There has been very little effort put towards validating simulated changes in surface albedo of different land cover by global land models, largely because of large uncertainties in the LULCC datasets and the large errors in simulated canopy LAI (Davin *et al* 2007, Park and Jeong 2021) and snow cover. For example, the latest land use change data by the ESMs for the CMIP6 experiments have a spatial resolution of 0.25° by 0.25° globally (Hurtt *et al* 2020), albeit multiple high spatial resolution land cover products at a global scale exist (e.g. Hansen *et al* 2013, Friedl and Sulla-Menashe 2022). These have been used to model land surface properties such as temperature (Su *et al* 2023), ecosystem production, and energy fluxes (Ouyang *et al* 2022, Li *et al* 2023) and others. Unfortunately, land cover change (LCC), such as forest degradation and forest fragmentation at finer spatial scales, can account for a significant fraction of global LCC but are not included in those global datasets. Therefore, it is very likely that ESMs are significantly underestimating $RF_{\Delta\alpha}$. Recent initiatives highlight a growing interest in integrating ground measurements, remote sensing images, and ESMs to achieve spatially and temporally continuous estimates of $RF_{\Delta\alpha}$, $GWI_{\Delta\alpha}$ and actual temperature changes (Davin *et al* 2007, IPCC 2022, Ouyang *et al* 2022). For example, the International Land Model Benchmarking (ILAMB) project aims to improve the performance of land models through systematic evaluation (Collier *et al* 2018).

Thus, one of the most critical pieces to the puzzle is to compare and potentially harmonize the determination of $RF_{\Delta\alpha}$ with the different methods mentioned. Here, we summarize what we have learned

from several case studies conducted in an agriculture-forest-mosaic region in southwestern Michigan. First, different approaches can generate deviated surface reflectivity due to their temporal mismatch, even over relatively homogeneous areas. For example, through *in situ* measurements, Miller *et al* (2016) and Lei *et al* (2023, 2024) observed comparable surface reflectance of 0.18–0.20 and 0.21–0.23 over a growing season at a sufficiently large corn field, which led to similar $RF_{\Delta\alpha}$ cooling of approximately -5.5 W m^{-2} when converted to a switchgrass landscape. Using Landsat and Sentinel satellite observations, Starr *et al* (2020), Carrer *et al* (2018), Shao *et al* (2014), and Bsaibes *et al* (2009) also observed similar surface reflectance over the study areas. However, as these orbiting satellites only provide a snapshot of local time at approximately 10:00–10:30 h, $RF_{\Delta\alpha}$ and GWI$\Delta\alpha$ based on satellite measurements are biased compared to those from the continuous *in situ* measurements (Cai *et al* 2016, He *et al* 2018, Sieber *et al* 2019, Sciusco *et al* 2022). Second, surface heterogeneity, particularly at or below measurements' detectable resolutions, can give biased albedo and hence the RF derivations. Plot- and field-scale measurements usually have fields of view over a single land cover, while satellites or ESMs are often complicated by mixed land cover within each pixel (panel). Sciusco *et al* (2020), Sciusco *et al* (2022)) found that RF varied significantly from 1.2 W m^{-2} to 5.2 W m^{-2} due to the various composition of croplands and forests within the landscapes across five ecoregions. Using both field and satellite observations, Bright and Lund (2021) noted that two adjacent fields planted with different sorghum varieties had distinct albedo up to 0.055, equating to a RF cooling of -4.1 W m^{-2} during the growing season and -1 W m^{-2} annually. At global scale, Davin *et al* (2007) found that LCC is responsible for a RF of -0.29 W m^{-2} during 1860–1992, but of -0.7 W m^{-2} for1992–2100. In conclusion, reducing the uncertainty of $RF_{\Delta\alpha}$ must consider specific LULC conversions, spatial scale and extent, and observation and model assumptions.

4. Global implications

GWI$_{\Delta\alpha}$ from LULCC allows us to create a more complete assessment of the biophysical potential of land-based climate mitigation. This becomes particularly important considering that current carbon-equivalent credits for mitigating land management practices account for mainly changes in CO_2, CH_4, and N_2O emissions, despite the potential importance of GWI$_{\Delta\alpha}$ (e.g. Salisbury *et al* 2023). While most documented ecosystem conversions have shown cooling effects on climate (along with other cooling mechanisms such as changes in evapotranspiration; Davin *et al* 2007), certain conversions in various geographies can lead to additional warming effects due to reduced albedo. For example, converting multi-layered forests into single layer croplands or prairies (Lei *et al* 2023, 2024) at high latitudes can increase albedo, but warming effects are observed with the establishment of poplar tree plantations in arid and semi-arid regions of northern Eurasia (Chen *et al* 2018). Thus, the perception of croplands as contributors to cooling effects should be evaluated in the context of local landscapes. For instance, croplands and afforested ecosystems in arid and semi-arid regions reflect less solar radiation compared to grasslands and deserts, thereby potentially increasing GWI through land conversions in these areas. Indirect LULCC effects can also have impact. For example, black carbon deposited on alpine glaciers, from forest burning, can substantially and extensively decrease glacier albedo, thereby accelerating climate-change induced melting (Bøggild *et al* 2009).

Long-term measurements of albedo for seven bioenergy crops at KBS LTER have revealed significant GWI$_{\Delta\alpha}$ when compared to historical forest cover. For example, in 2021, all seven crops exhibited higher average annual albedo than the forest, with average values of 0.095 in the growing season and 0.193 in non-growing season (figure 4(a)). As a result, conversion of forest to crops produced cooling effects on climate, with GWI$_{\Delta\alpha}$ equivalent to -1.24 and -1.70 Mg C ha^{-1} yr^{-1}. This contrasts with expected soil C sequestration potentials of -0.3 to -1.0 Mg C ha^{-1} yr^{-1} for the 30–50 years following conversion from annual row crops (Gelfand *et al* 2013). A contrast with the long-term net ecosystem productivity (NEP) of aggrading forests in the region ($\sim$2.5 Mg C ha^{-1} yr^{-1}; Gough *et al* 2008, Xie *et al* 2014) further underscores the magnitude of this impact, with the GWI$_{\Delta\alpha}$ of the seven crops at KBS accounting for 48%–57% of regional forest NEP values (figure 4(b)).

The inclusion of changes in albedo, quantified as GWI$_{\Delta\alpha}$, in full-cost GHG accounting assessments of changes in land use and cropping practices (e.g. Robertson *et al* 2000, Gelfand *et al* 2013) provides an opportunity to avoid or promote, as appropriate, practices that result in albedo change in the same way that current assessments inform GHG impacts. Current assessments of the potential for land-based solutions to climate mitigation (e.g. Robertson *et al* 2022, Pett-Ridge *et al* 2023) do not include the potential for management changes contributing to significant mitigation by altering cropland or grazing land albedo. Yet practices like surface residue retention by delayed tillage or no-till could maintain a higher albedo during the non-growing season due to crop residue's greater surface reflectivity than bare soil, and in northern climates due to the greater capacity of residue-covered soil to retain snow cover (Qiu *et al* 2022). That relatively small changes in albedo can result in significant GWI$_{\Delta\alpha}$ differences—in the KBS
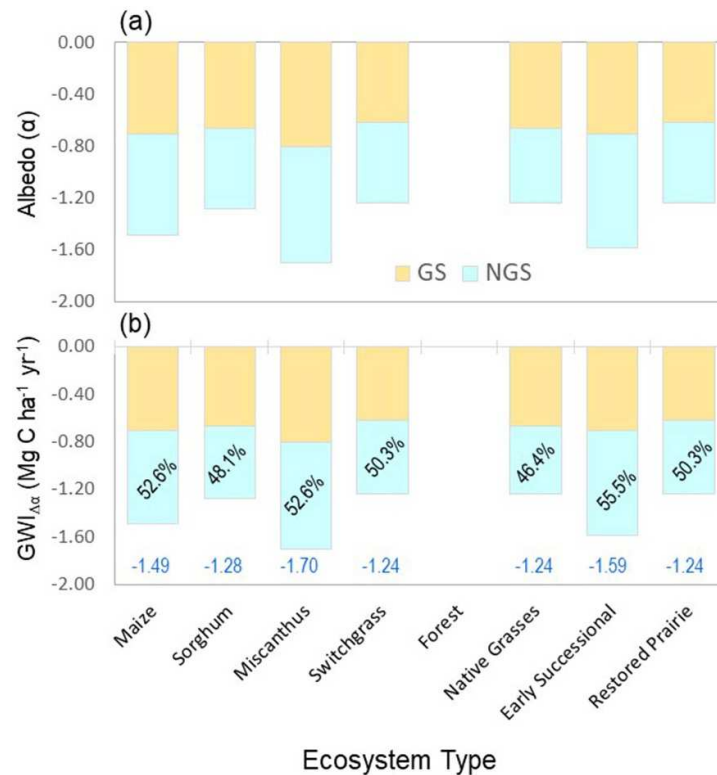
Figure 4. (a) The average land surface albedo ($\Delta\alpha$) during the growing season (GS) and non-growing season (NGS) was measured for eight major ecosystem types in southwestern Michigan in 2021. (b) The global warming potential due to albedo differences (GWI$_{\Delta\alpha}$) was assessed for the native temperate forest ecosystem in the same region.

case up to 25% differences among cropping systems (figure 4(b))—and that GWI$_{\Delta\alpha}$ can be of similar magnitude to soil carbon change—suggests a capacity for mitigation largely unrecognized.

According to the GlobCover 2009 database (**SI-3**), croplands cover 15.5% of terrestrial biomes. This implies a significant capacity for albedo cropland management to contribute to climate change mitigation globally. Carrer *et al* (2023) suggest that by extending the introduction of cover crops to all possible fallow periods in Europe, the mitigation potential through albedo effects could be as great as 1.838 Mt C yr^{-1}. Globally, assuming GWI$_{\Delta\alpha}$ values of 0.1 and 0.5 Mg C ha^{-1} yr^{-1}, from 0.227 Gt C yr^{-1} to 1.135 Gt C yr^{-1} could be credited to cover crops globally, considering that certain croplands may have warming effects and that GWI$_{\Delta\alpha}$ varies significantly depending on biome, geographic location, management practices, and other factors outlined in section 2. The most recent global carbon budget indicated a land uptake of carbon at 3.4 Gt C yr^{-1} (Friedlingstein *et al* 2020). Albedo management might therefore be equivalent to 7%–33% of the contemporary terrestrial carbon sink. This amount of carbon equivalent credit or debt should be included in calculations of the total GWI of a land parcel (e.g. Gelfand *et al* 2011, Cai *et al* 2016).

5. Outlooks

We provide an overview of the physical foundations for estimating GWI$_{\Delta\alpha}$ and highlight the shortcomings in current data and methodologies when assessing the significance of GWI$_{\Delta\alpha}$ for achieving a comprehensive estimate of terrestrial ecosystem GWI. Although there has been limited utilization of available *in situ* measurements and satellite data, various means such as drone, airborne, satellite, and ESMs technologies can enhance our knowledge on LULCC on albedo, RF and GWI$_{\Delta\alpha}$. Results from a site in southwest Michigan USA demonstrate that GWI$_{\Delta\alpha}$ can be substantial, exceeding the values reported in AR6 of the IPCC. Similar conclusions regarding the influence of albedo changes resulting from land use and LCCs on GWI have been supported by evidence from Europe (e.g. Carrer *et al* 2013, Carrer *et al* 2018), and we conclude that GWI$_{\Delta\alpha}$ are significantly underestimated in the last three IPCC assessment reports. Recent findings have also shown that the influence of albedo changes upon conversion of maize cropland to perennial bioenergy crops is of the same climate-mitigating effect as soil carbon accumulation following conversion from annual croplands. We propose the inclusion of GWI$_{\Delta\alpha}$ in policy to ensure that landowners receive appropriate carbon credits.

This approach would account for the broader impact of albedo changes on GWI, encouraging sustainable land management practices that increase albedo.

To include $GWI_{\Delta\alpha}$ for a holistic assessment of total GWI at local landscapes, as well as for forecasting future climate (e.g. IPCC efforts), considering continued and intensified LCCs, we propose the following research priorities. These priorities aim to enable the estimation of the three key parameters (i.e. $\Delta\alpha$, T_a, T_k) for quantifying $GWI_{\Delta\alpha}$ (equation (1)) of a land parcel:

- Promoting a comprehensive global albedo database by compiling existing measurements (e.g. FLUXNET, ICOS, USCCC) and increasing monitoring sites in underrepresented land cover types and regions. This effort should also include atmospheric transmittance (T_a) of different cloud covers.
- Developing regional networks of reference sites with measured albedo over time to accurately quantify changes in albedo ($\Delta\alpha$) due to land cover and land use changes. This involves the challenge of constructing accurate pre- and post-LCC assessments at local landscapes.
- Enhancing current algorithms in remote sensing of albedo by integrating geostationary and other orbital satellites to accurately estimate continuous albedo values under various weather conditions for local landscapes. Commercial missions of more frequent overpasses throughout the day shall be encouraged. Empirical modeling of diurnal albedo changes from satellite snapshots (e.g. Landsat, Sentinel, MODIS) can be achieved by integrating multiple satellite bands with *in situ* measurements of incoming solar radiation, often available at weather stations and flux towers. Atmospheric transmittance of outgoing radiation (T_k) should be explored by comparing satellite measurements of reflectance (including from clouds) with ground records of outgoing radiation. Utilizing drone technology equipped with pyranometers can effectively scale up ground measurements to satellite-based albedo estimation across multiple land cover types.
- Constructing a $GWI_{\Delta\alpha}$ component by integrating multiple data sources (e.g. *in situ* measurements of albedo, satellite records, land cover maps, weather conditions) and use these estimates and high spatial resolution data of land use change to derive $GWI_{\Delta\alpha}$ at the spatial resolution of ESMs for use in model benchmarking, such as ILAMB. Identifying reference cover types as well as accounting for the divergent changes in albedo over time by cover type within a panel is essential for incorporating $GWI_{\Delta\alpha}$ into a holistic carbon trading market for landowners.

ORCID iDs

Jiquan Chen ⬤ https://orcid.org/0000-0003-0761-9458
Cheyenne Lei ⬤ https://orcid.org/0000-0002-7274-6309
Pietro Sciusco ⬤ https://orcid.org/0000-0001-7640-4472

References

Abraha M, Chen J Q, Hamilton S K, Sciusco P, Lei C, Shirkey G, Yuan J and Robertson G P 2021 Albedo-induced global warming impact of conservation reserve program grasslands converted to annual and perennial bioenergy crops *Environ. Res. Lett.* **16** 084059

Bøggild C E, Solberg R and Hodson A J 2009 Aerosol deposition on glaciers and resulting melting from darkening *IOP Conf. Ser.: Earth Environ. Sci.* **6** 012005

Bonan G B 1996 Sensitivity of a GCM simulation to subgrid infiltration and surface runoff *Clim. Dyn.* **12** 279–85

Bright R M, Davin E, O'Halloran T, Pongratz J, Zhao K and Cescatti A 2017 Local temperature response to land cover and management change driven by non-radiative processes *Nat. Clim. Change* **7** 296–302

Bright R M and Lund M T 2021 CO_2-equivalence metrics for surface albedo change based on the radiative forcing concept: a critical review *Atmos. Chem. Phys.* **21** 9887–907

Bright R M, Myhre G, Astrup R, Antón-Fernández C and Strømman A H 2015 Radiative forcing bias of simulated surface albedo modifications linked to forest cover changes at northern latitudes *Biogeosciences* **12** 2195–205

Bsaibes A *et al* 2009 Albedo and LAI estimates from FORMOSAT-2 data for crop monitoring *Remote Sens. Environ.* **113** 716–29

Burakowski E, Tawfik A, Ouimette A, Lepine L, Novick K, Ollinger S, Zarzycki C and Bonan G 2018 The role of surface roughness, albedo, and bowen ratio on ecosystem energy balance in the eastern united states *Agric. For. Meteorol.* **249** 367–76

Cai H, Wang J, Feng Y, Wang M, Qin Z and Dunn J B 2016 Consideration of land use change-induced surface albedo effects in life-cycle analysis of biofuels *Energy Environ. Sci.* **9** 2855–67

Carrer D, Moparthy S, Lellouch G, Ceamanos X, Pinault F, Freitas S C and Trigo I F 2018 Land surface albedo derived on a ten daily basis from meteosat second generation observations: the NRT and climate data record collections from the EUMETSAT LSA SAF *Remote Sens.* **10** 1262

Carrer D, Roujean J L, Lafont S, Calvet J C, Boone A, Decharme B, Delire C and Gastellu-Etchegorry J P 2013 A canopy radiative transfer scheme with explicit FAPAR for the interactive vegetation model ISBA-A-gs: Impact on carbon fluxes *J. Geophys. Res. Biogeosci.* **118** 888–903

Carrer M, Dibona R, Prendin A L and Brunetti M 2023 Recent waning snowpack in the alps is unprecedented in the last six centuries *Nat. Clim. Change* **13** 155–60

Ceamanos X, Moparthy S, Carrer D and Seidel F C 2019 Assessing the potential of geostationary satellites for aerosol remote sensing based on critical surface albedo *Remote Sens.* **11** 2958

Chen D, Loboda T V, He T, Zhang Y and Liang S 2018 Strong cooling induced by stand-replacing fires through albedo in siberian larch forests *Sci. Rep.* **8** 4821

Chen J 2021 *Biophysical Models and Applications in Ecosystem Analysis. Biophysical Models and Applications in Ecosystem Analysis* (Higher Education Press)

Chu H, Baldocchi D D, John R, Wolf S and Reichstein M 2017 Fluxes all of the time? A primer on the temporal representativeness of FLUXNET *J. Geophys. Res. Biogeosci.* **122** 289–307

Collier N, Hoffman F M, Lawrence D M, Keppel-Aleks G, Koven C D, Riley W J, Mu M and Randerson J T 2018 The international land model benchmarking (ILAMB) system: design, theory, and implementation *J. Adv. Model. Earth Syst.* **10** 2731–54

Davin E L, de Noblet-ducoudré N and Friedlingstein P 2007 Impact of land cover change on surface climate: relevance of the radiative forcing concept *Geophys. Res. Lett.* **16** L13702

Friedl M and Sulla-Menashe D 2022 MODIS/Terra+Aqua Land Cover Type Yearly L3 Global 0.05Deg CMG V061 (NASA EOSDIS Land Processes DAAC) (https://doi.org/10.5067/MODIS/MCD12C1.061)

Friedlingstein P *et al* 2020 Global carbon budget 2020 *Earth Syst. Sci. Data* **12** 3269–340

Gelfand I, Sahajpal R, Zhang X, Izaurralde R C, Gross K L and Robertson G P 2013 Sustainable bioenergy production from marginal lands in the US Midwest *Nature* **493** 514–7

Gelfand I, Zenone T, Jasrotia P, Chen J, Hamilton S K and Robertson G P 2011 Carbon debt of Conservation Reserve Program (CRP) grasslands converted to bioenergy production *Proc. Natl Acad. Sci.* **108** 13864–9

Ghimire B, Williams C A, Masek J, Gao F, Wang Z, Schaaf C and He T 2014 Global albedo change and radiative cooling from anthropogenic land cover change, 1700–2005 based on MODIS, land use harmonization, radiative kernels, and reanalysis *Geophys. Res. Lett.* **41** 9087–96

Gough C M, Vogel C S, Schmid H P, Su H B and Curtis P S 2008 Multi-year convergence of biometric and meteorological estimates of forest carbon storage *Agric. For. Meteorol.* **148** 158–70

Graf A *et al* 2023 Joint optimization of land carbon uptake and albedo can help achieve moderate instantaneous and long-term cooling effects *Commun. Earth Environ.* **4** 298

Hansen M C *et al* 2013 High-resolution global maps of 21st-century forest cover change *Science* **342** 850–3

He T, Wang D and Qu Y 2018 Land surface albedo *Comprehensive Remote Sensing* (Elsevier)

Hurtt G C *et al* 2020 Harmonization of global land use change and management for the period 850–2100 (LUH2) for CMIP6 *Geosci. Model. Dev.* **13** 5425–64

IPCC (Intergovernmental Panel on Climate Change) 2001 *Climate Change 2001: The Scientific Basis. Contribution of Working Group I to the Third Assessment Report of the Intergovernmental Panel on Climate Change* (Cambridge University Press)

IPCC (Intergovernmental Panel on Climate Change) 2022 *Climate Change 2022: Impacts, Adaptation, and Vulnerability. Contribution of Working Group II to the Sixth Assessment Report of the Intergovernmental Panel on Climate Change* (Cambridge University Press)

Jarvis P 1976 The interpretation of the variations in leaf water potential and stomatal conductance found in canopies in the field *Phil. Trans. R. Soc. B* **273** 593–610

Jenkins S, Millar R J, Leach N and Allen M R 2018 Framing climate goals in terms of cumulative CO_2-forcing-equivalent emissions *Geophys. Res. Lett.* **45** 2795–804

Lawrence D M *et al* 2019 The community land model version 5: description of new features, benchmarking, and impact of forcing uncertainty *Adv. Model. Earth Syst.* **11** 4245–87

Lee X *et al* 2011 Observed increase in local cooling effect of deforestation at higher latitudes *Nature* **479** 384–7

Lei C, Chen J, Ibanez I, Sciusco P, Shirkey G, Lei M, Reich P and Robertson G P 2024 Albedo of crops as a nature-based climate solution to global warming *Environ. Res. Lett.* **19** 084032

Lei C, Chen J and Robertson G P 2023 Climate cooling benefits of cellulosic bioenergy crops from elevated albedo *Glob. Change Biol. Bioenergy* **15** 1373–86

Li F, Xiao J, Chen J, Ballantyne A, Jin K, Li B, Abraha M and John R 2023 Global water use efficiency saturation due to increased vapor pressure deficit *Science* **381** 672–77

Masson-Delmotte V *et al* 2021 *Climate Change 2021: The Physical Science Basis. Contribution of Working Group I to the Sixth Assessment Report of the Intergovernmental Panel on Climate Change, 2* (Cambridge University Press) (https://doi.org/10.1017/9781009157896)

Miller J N, VanLoocke A, Gomez-Casanovas N and Bernacchi C J 2016 Candidate perennial bioenergy grasses have a higher albedo than annual row crops *GCB Bioenergy* **8** 818–25

Ouyang Z T *et al* 2022 Albedo changes caused by future urbanization contribute to global warming *Nat. Commun.* **13** 3800

Park H and Jeong S 2021 Leaf area index in earth system models: how the key variable of vegetation seasonality works in climate projections *Environ. Res. Lett.* **16** 034027

Pett-Ridge J *et al* 2023 *Roads to Removal: Options for Carbon Dioxide Removal in the United States* (Lawrence Livermore National Laboratory (LLNL))

Qiu H, Huggins D R, Wu J Q, E. Barber M, K. Mccool D and Dun S 2022 Residue management impacts on field-scale snow distribution and soil water storage *Trans. ASABE* **54** 1639–47

Robertson G P, Hamilton S K, Paustian K and Smith P 2022 Land-based climate solutions for the United States *Glob. Change Biol.* **28** 4912–9

Robertson G P, Paul E A and Harwood R R 2000 Greenhouse gases in intensive agriculture: contributions of individual gases to the radiative forcing of the atmosphere *Science* **289** 1922–5

Salisbury J, Hu X, Speed J D M, Iordan C M, Austrheim G and Cherubini F 2023 Net climate effects of moose browsing in early successional boreal forests by integrating carbon and albedo dynamics *J. Geophys. Res. Biogeosci.* **128** e2022JG007279

Schaaf C B *et al* 2002 First operational BRDF, albedo nadir reflectance products from MODIS *Remote Sens. Environ.* **83** 135–48

Sciusco P, Chen J Q, Abraha M, Lei C, Robertson G P, Lafortezza R, Shirkey G, Ouyang Z, Zhang R and John R

2020 Spatiotemporal variations of albedo in managed agricultural landscapes: inferences to global warming impacts (GWI) *Landsc. Ecol.* **35** 1385–402

Sciusco P, Chen J Q, Giannico V, Abraha M, Lei C, Shirkey G, Yuan J and Robertson G P 2022 Albedo-induced global warming impact at multiple temporal scales within an upper Midwest USA watershed *Land* **11** 283

Sellers P J 1985 Canopy reflectance, photosynthesis and transpiration *Int. J. Remote Sens.* **6** 1335–72

Shao C, Li L, Dong G and Chen J 2014 Spatial variation of net radiation and its contribution to energy balance closures in grassland ecosystems *Ecol. Process.* **3** 1–11

Sieber P, Ericsson N and Hansson P A 2019 Climate impact of surface albedo change in life cycle assessment: implications of site and time dependence *Environ. Impact Asses.* **77** 191–200

Smith C J *et al* 2020 Effective radiative forcing and adjustments in cmip6 models *Atmos. Chem. Phys.* **20** 9591–618

Starr J, Zhang J, Reid J S and Roberts D C 2020 Albedo impacts of changing agricultural practices in the United States through Space-Borne analysis *Remote Sens.* **12** 2887

Su Y *et al* 2023 Asymmetric influence of forest cover gain and loss on land surface temperature *Nat. Clim. Change* **13** 823–31

Tian L, Chen J Q and Shao C L 2018 Interdependent dynamics of LAI-albedo across the roofing landscapes: mongolian and tibetan plateaus *Remote Sens.* **10** 1159

Tian L, Chen J Q and Zhang Y J 2017 Growing season carries stronger contributions to albedo dynamics on the Tibetan plateau *PLoS One* **12** e0180559

Wang Z *et al* 2017 Monitoring land surface albedo and vegetation dynamics using high spatial and temporal resolution synthetic time series from Landsat and the MODIS BRDF/NBAR/albedo product *Int. J. Appl. Earth Obs. Geoinf.* **59** 104–17

Xiao J *et al* 2008 Estimation of net ecosystem carbon exchange for the conterminous united states by combining MODIS and AmeriFlux data *Agric. For. Meteorol.* **148** 1827–47

Xie J, Chen J, Sun G, Chu H, Noormets A, Ouyang Z, John R, Wan S and Guan W 2014 Long-term variability and environmental control of the carbon cycle in an oak-dominated temperate forest *For. Ecol. Manage.* **313** 319–28

Xu K M, Li Z J, Cheng A N and Hu Y 2020 Changes in clouds and atmospheric circulation associated with rapid adjustment induced by increased atmospheric CO_2: a multiscale modeling framework study *Clim. Dyn.* **55** 277–93

Zhu Q, Chen J and Charles P 2024a Albedo-induced global warming potential following disturbances in global temperate and boreal forests *J. Geophys. Res. Biogeosci.* **129** e2023JG007848

Zhu Q, Chen J, Wu L, Huang Y, Shao C, Dong G, Xu Z and Li X 2024b Changes in albedo and its radiative forcing of grasslands in East Asia drylands *Ecol. Process.* **13** 1–5